



Received on 24 August 2019; received in revised form, 05 February 2020; accepted, 09 March 2020; published 01 August 2020

TERBINAFINE LOADED CHITOSAN SCAFFOLD FOR FUNGAL WOUND TREATMENT

Roshan Prasad Yadav* and Meenakshi K. Chauhan

Department of Pharmaceutics, Delhi Institute of Pharmaceutical Sciences and Research (DIPSAR), Delhi - 110017, New Delhi, India.

Keywords:

Chitosan scaffold, Drug release, Physical characterization, Tissue engineering, Fungal wound healing

Correspondence to Author:

Mr. Roshan P. Yadav

Research Scholar,
Department of Pharmaceutics,
Delhi Institute of Pharmaceutical
Sciences and Research (DIPSAR),
Delhi - 110017, New Delhi, India.

E-mail: roshanyadavxyz@gmail.com

ABSTRACT: Chitosan-based porous scaffolds are of great interest in biomedical applications especially in tissue engineering because of their excellent biocompatibility in vivo, good texture, surface contact, controllable degradation rate and tailorable mechanical properties. These days biomaterials scaffolds have contributed as an alternative choice of therapy mainly due to the increase failure rates in autografts and allografts techniques. Terbinafine HCl is allylamines group of drugs which is used topically to treat dermatophyte group of fungi like ringworm. Chitosan possesses both anti-bacterial and antifungal property which synergises with Terbinafine HCl (TBH) for both prophylactic and therapeutic actions in treating fungal wound infection (FWI). The haemostatic property of chitosan allows sorption of plasma, erythrocyte coagulation and platelets activation. These properties contribute additional role in repairing debilitated tissue. The prolong drug release property of fabricated scaffold and its natural characteristics of remodelling tissue favours its use in human fungal wound dressing. The main intention of this research work is to fabricate stable polymer medical devices, examine drug release profile and characterize TBH loaded CS porous scaffold with improved dual bioactivity against fungal wound infection. In the present research study it was observed that the fabricated scaffold had a prolonged drug release in compare to available conventional marketed cream, acceptable drug-polymer compatibility and hence can be projected that natural property of chitosan polymer favours synergistic effect in healing fungal wounded skin that attributed to sort out the problem of repeated use of drug application.

INTRODUCTION: Skin tissue defects and diseases due to the consequence of infections due to bacteria or fungi and degenerative loss are of major concern in the field of human health¹. The current clinical option for repairing skin defects and diseases is skin grafting, which is classified as autografts and allografts².

Failure rates in these techniques are attributed to several reasons like disease transfer, immune rejection, and donor crisis^{3,4}. This has prompted a lot of research interest among the scientific community for an alternative solution⁵.

In this context, skin tissue engineering has emerged as an alternative strategy to repair and/or replace diseased and/or damaged skin tissue through the development of a biologically active substitute so-called tissue-engineered scaffold that offers complete recovery of original state and skin tissue function⁶. Chitosan is a natural alternate biopolymer which is considered as an ideal biomaterial due to its excellent biocompatibility,

QUICK RESPONSE CODE 	DOI: 10.13040/IJPSR.0975-8232.11(8).3806-18
	This article can be accessed online on www.ijpsr.com
DOI link: http://dx.doi.org/10.13040/IJPSR.0975-8232.11(8).3806-18	

abundant availability, intrinsic antibacterial property, and biodegradability^{7, 8}. Hence, the present research focuses on the development of CS-based 3D matrices composite with Terbinafine HCl by lyophilization method to mimic the unique hierarchical architecture of tissue matrix as well to ensure the prolonged release of drugs that are being incorporated. A scaffold is a temporary matrix which behaves as a topical patch and aids in the proliferation of cells until they reanimate the tissue. Scaffolds hence degrade after a certain period, permitting the formation of new tissue and healing the infected wound.

Scope and Objectives: In recent years, skin tissue engineering has emerged as the most promising technique for the treatment of skin tissue defects and diseases through the development of a biologically active 3D artificial extracellular matrix so-called tissue-engineered scaffold. The design and fabrication of such 3D porous scaffolds with a desired set of properties is a key challenge. Among the various biopolymers explored for tissue engineering applications, chitosan is considered as one of the universal and potential candidates owing to its biocompatibility, biodegradability, and wound healing properties⁹. However, chitosan produce desired antifungal bioactivity. Therefore, the present research focuses on the development of a novel chitosan-based composite TBH porous scaffold with the purpose of preventing fungal induced wound infection and alternative choice of wound healing with or without fungal infection. The specific objectives of this research work are:

- To develop TBH loaded CS porous scaffolds with improved dual bioactivity against fungal wound infection.
- To improve the supportive cell property of the developed composite scaffolds by conjugation with a bioactive molecule.
- To study the physicochemical and mechanical properties of the scaffold.
- To develop scaffolds with controlled biodegradation property.
- To examine its *in-vitro* release behaviors.

Properties of Scaffold:

Should be Porous: The pore size varies depending on specific tissue engineering applications such as skin tissue (50-300 µm)^{10, 11}. The scaffold should

have optimum porosity to facilitate nutrient and active ingredients diffusion and allow cell migration. It should not be highly porous, which ultimately decreases the mechanical strength of the scaffold^{12, 13}.

Biodegradable & Biocompatible: The rate of degradation should match with the rate of new tissue formation without the release of any toxic by-products. Furthermore, the scaffold should not solubilize rapidly during the tissue regeneration process^{14, 15}.

Have Bioactivity: Bioactivity Scaffold should form and deposit apatite crystals in both *in-vitro* and *in-vivo* environments¹⁶.

Possess Hydrophilicity: Reports suggest higher hydrophilic surfaces of scaffold matrices are responsible for improved cellular attachment, whereas relatively hydrophobic surfaces are essential for improved protein adsorption^{17, 18}.

Hemostatic: The hemostatic properties of chitosan polymer is mainly due to in build the positive charge, which allows to mucoadhesion with the negative charge of mucus. This allows the sorption of plasma and coagulation erythrocyte along with adhesion aggregation and activation of the platelet. These proceeds smooth muscle formation.

Bactericidal: Due to electrostatic interaction between positive charges of chitosan microbial cell membrane causes membrane wall permeability and hydrolysis of the peptidoglycan in micro-organism. Its degradation product, chitoligo-saccharide has antimicrobial effect for the various MO.

Anti-inflammatory: Immune the response to biopolymer material leads to aggregation of monocyte at the inflammation site. This monocyte gets matured macrophages and results in secreting various anti-inflammatory cytokines like IL-10, which act as a healing factor.

MATERIALS AND METHODS: Low molecular weight chitosan (molecular weight 50-190 kDa, degree of deacetylation 75-85%) was purchased from Sigma-Aldrich. Acetic acid (glacial) 100%. Terbinafine HCl pure drug was obtained as a gift sample from Shilpa Medicare Ltd, Raichur, and Karnataka. DMSO and Methanol (HPLC Grade)

were products from Merck. Tween 80 and Dialysis bag membrane (molecular weight cut-off 12400) to perform *in-vitro* release study were purchased from Sigma–Aldrich Co., USA. Sodium hydroxide and Lysozyme for biodegradation studies were obtained from Sigma-Aldrich, USA. The chemicals used for preparing phosphate buffer saline and simulated body fluid (SBF) were products from Qualigens, Thermo Fischer Scientific, and India. Other reagents used in this experiment were all of the analytical grades. The statistical analysis data were expressed as mean \pm standard deviation with $n = 3$.

The Scheme of scaffold development and its evaluation are as follow:

Drug Standardization:

Identification of TBH by IR Spectrum:

Identification of Terbinafine Hydrochloride Infra-red spectrum The I.R. absorption spectrum of Terbinafine Hydrochloride sample should coincide with the I.R. absorption spectrum of standard Terbinafine Hydrochloride¹⁹. This test gives the authenticity of the compound.

Solubility Studies: For crude solubility, the equivalent amount of the drug was taken in different test tubes containing the different solvents. Test tubes were shaken vigorously after the addition of each portion of solvent and then crude solubility was observed by visual inspection¹⁹.

UV Spectrophotometric Analysis: Spectral analysis was made on Shimadzu UV-1800, which was employed with wavelength range: 400 to 200 nm., Scan Speed: 40 nm/min., Photometric accuracy: ± 0.003 . All the glassware was rinsed

thoroughly with double distilled water and dried in hot air oven¹⁹. The standard stock solution was prepared by weighing 10 mg of standard Terbinafine HCl and transferred to a 10 ml volumetric flask containing a mixture of 5 ml methanol and 5 ml water. Hence, the stock solution of 1000 $\mu\text{g/ml}$ was prepared¹⁹. After all 3 - 15 $\mu\text{g/ml}$ solutions of Terbinafine Hydrochloride were prepared in 50% aqueous methanol, and spectrum was recorded between 200-400 nm. Spectrums for above concentration were obtained with $n = 3$. The overlain derivative spectrum of Terbinafine Hydrochloride at different concentrations was recorded at 283 nm, and the calibration curve for Terbinafine HCl has plotted along with the determination of straight-line equation¹⁹.

Preparation CS/TBH Composite Scaffolds:

Terbinafine HCl (TBH) powder in micro and nano-size was dispersed in a mixture of HPLC graded methanol, water, and DMSO in the ratio 50:45:5 by ultra-sonication. On the other side, CS was dissolved in aqueous acetic acid solution with a ratio of either 99:1, 97:3, or 95:5 to form 2.5% wt/v of polymer solution²⁰. The prepared TBH solution was added to the chitosan solution drop by drop and allowed to stir overnight until homogeneity is achieved¹⁶. After this, Solution was poured in petri dish and kept at $-20\text{ }^{\circ}\text{C}$ for 6 h. Than immersed the petridish in pre-cooled NaOH: EtOH (70:30 v/v) solution and frozen at $-20\text{ }^{\circ}\text{C}$ for 6 hours. After this, it was dried in a freeze drier for 6 to 8 h at $-80\text{ }^{\circ}\text{C}$. The obtained composite scaffolds were cut into specific dimensions and made ready for different characterization techniques²¹. The **Fig. 1a & b** show a 3D image of laboratory prepared chitosan/TBH composite scaffold.

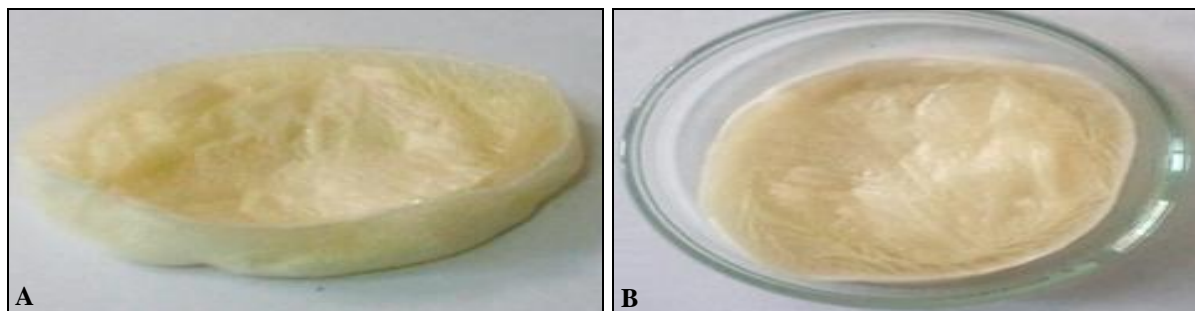


FIG. 1A & B: SHOW 3D IMAGE OF LABORATORY PREPARED CHITOSAN/TBH COMPOSITE SCAFFOLD

Characterization of Scaffolds:

Measurement of pH: The apparent pH of the chitosan composite TBH solution was determined

using pH meter (pH Tutor Bench Meter, HANNA instruments, Singapore). The gel formulation (100 mg) was weighed in a 50 mL volumetric flask, and

then volume was made up with distilled water to 50 mL. The pH of the dispersion was measured²².

Rheological Behaviour's: The viscosity of pure CS and CS/TBH composite solutions was analyzed by Brookfield viscometer (Brookfield engineering laboratories, Inc., MA, USA) with spindle no. 6 at 10 rpm at a temperature of 37 ± 0.5 °C^{23, 24}.

Thermal Characterization: The thermal stability of the scaffold was assessed using DSC under N₂ atmosphere at a heating rate of 10 °C/min. Thermo Gravimetric Analyzer was used to obtain the pyrolytic pattern of the samples under N₂ atmospheric at a heating rate of 10 °C/min²⁶. For calorimetric measurements, standard aluminum pans with accurately weighed 1-2 mg samples were tightly sealed. Samples were heated at a scanning rate of 10 °C/min over a temperature range between 40 °C and 400 °C. An empty pan was maintained by purging with nitrogen²³.

Thickness & Diameter of scaffolds: Thickness and Diameter of scaffolds were measured by Digital Vernier Caliper (150 mm). Three parallel sets were analyzed for each character, and the mean value of the thickness and diameter were noted²⁷.

Morphology: (Scanning Electron Microscopy): Scanning Electron Microscopy (SEM) was performed using a JEOL-JSM 6480 LV to observe the morphology of developed CS-based TBH composite scaffolds. Thin discs of equivalent 1 mm thickness were cut from the scaffolds using a surgical scalpel. The traces of moisture present in the scaffolds were removed by drying in a vacuum drier for 2 h at 40 °C. The platinum coating was done before imaging.

A minimum of 25 pores was considered for calculating the pore size of the developed scaffolds by using Image J (USA) software²⁸.

Porosity Measurement: The total porosity was determined by the liquid displacement method. Initially, the volume of the ethanol was taken. Then the scaffold was immersed into the dehydrated alcohol for 48 h until it was saturated by absorbing the alcohol, and then the volume of ethanol plus impregnated scaffold was noted. Finally, the porosity of the sample was calculated based on the following formula.

$$\text{Porosity (\%)} = (V_1 - V_3 / V_2 - V_3) \times 100$$

Where V_1 = Initial known volume of ethanol, V_2 = volume of the sum of ethanol and submerged scaffold sample, and V_3 = volume of ethanol after the removal of the scaffold sample. Three parallel sets were analyzed for every scaffold, and the mean value of the porosities of different scaffolds was achieved²⁸.

Apparent Density Analysis: The apparent densities of scaffolds were evaluated by calculating the ratio of the weight of lyophilized scaffold to their volume. The apparent density ρ was obtained from the equation.

$$\rho = W / \eta (D/2)2H$$

Where W is the weight of scaffold, η , is the pi-constant (value= 3.14), D , the diameter and H , the thickness (height) of scaffold²⁸.

Swelling Study: Scaffolds of equal weights in triplicates were immersed in 30 ml PBS (pH 7.4) at 37 °C. The scaffolds were retrieved at predetermined time-periods, and excess PBS removed using filter paper. The swollen scaffold weighed was recorded using an electronic balance (Sartorius-CP). The swelling ratio was calculated using the following formula²⁹.

$$\% \text{ Swelling} = [(W_{\text{ET}_{\text{wt}}} - DRY_{\text{wt}}) / DRY_{\text{wt}}] \times 100$$

Where $W_{\text{ET}_{\text{wt}}}$ and DRY_{wt} correspond to the swollen and dry weights of the scaffolds, respectively²⁸.

Water Retention Ability: To measure the water retention ability, scaffolds of equal weights in triplicates were immersed in 30 ml distilled water at 37 °C for 24 h. Then the scaffolds were gently removed from a beaker after 24 h and placed on a wire mesh rack. Excessive water was drained, and wet scaffolds were transferred to centrifuge tubes with filter paper at the bottom, centrifuged at 500 rpm for 3 min. and weighed immediately (W'_{wet}).

$$ER = [(W'_{\text{wet}} - W_{\text{dry}}) / W_{\text{dry}}] \times 100$$

Where W_{wet} and W_{dry} correspond to the swollen and dry weight of the scaffolds, respectively³⁰.

Functional Analysis (FTIR): Fourier transform infrared spectroscopy (FTIR) was performed to

evaluate the structural property and functional groups of the developed CS and CS-based composite scaffolds by using an Infrared Microscope [Shimadzu AIM-8800, Japan]. The hydraulic press was used to pelletize the scaffold samples by mixing them with dry KBr powder. The mixture was pressed into transparent disks and used for IR analysis. The machine was operated in transmittance mode by using the range 500 to 4000 cm^{-1} with a resolution of 8 cm^{-1} ¹⁰.

Optical Microscopy: Optical image of the scaffolds were obtained with the optical Binocular microscope (CTR 6000, Leica, Wetzlar, Germany) using fine focus only³¹.

In-vitro Biodegradation Study: *In-vitro* release of Terbinafine HCl from CS composite TBH scaffold was carried out using a dialysis bag membrane method. CS composite TBH scaffold suspended in 2 mL of phosphate buffer saline, pH 7.4 maintained at 37 °C was taken in dialysis tube (16 mm diameter), and both ends were tightly knotted. The dialysis bag membrane was then placed in 30 ml of SWF at pH 7.4 phosphate buffer containing 0.8% tween 80 solutions maintained at 37 °C with magnetically stirred at 200 rpm. At regular intervals of time, the supernatant was pipetted out and replaced with equivalent volumes of fresh phosphate buffer solution. The extent of drug release was subsequently evaluated by spectrometrically assayed for the drug concentration at λ_{max} 283 nm. The correction for cumulative dilution was calculated. The release studies were performed in triplicate³¹.

In-vitro Drug Release Study by using Dialysis Bag Membrane Method: *In-vitro* biodegradation study of the developed CS and CS-based composite scaffolds was performed by soaking them in PBS containing 500 $\mu\text{g ml}^{-1}$ of lysozyme. The initial dry weight of the scaffold samples was weighed and noted as W_I . The soaking time of the samples was 2, 7, 14, 21, 28, and 35 days. The samples were removed at regular time intervals and freeze-dried before calculating the final weight, W_F . The remaining weight % (W_R) was calculated according to the formula given below. All the experiments were performed in triplicate¹⁶.

$$\% \text{ Weight remaining } (W_R) = 100 - [(W_I - W_F) / W_I] \times 100$$

Where W_I = Initial weight of scaffold and W_F = Final weight after incubation

Statistical Analysis: Statistical differences were evaluated by the Tukey-Kramer test after one-way analysis of variance at $p < 0.05$ by using an online version of graph pad quick calc software. The statistical analysis data were expressed as mean \pm standard deviation with $n = 3$.

RESULTS AND DISCUSSION:

FTIR spectra of Terbinafine HCl: The drug sample was firstly identified spectroscopically by FTIR (Fourier transform infrared) with standard range. The result in **Fig. 2** & observation **Table 1** showed that the drug Terbinafine hydrochloride was pure and free from impurities because the value of the drug sample is within a standard range. Apart, white-colored physical appearances also ensure of Terbinafine HCl.

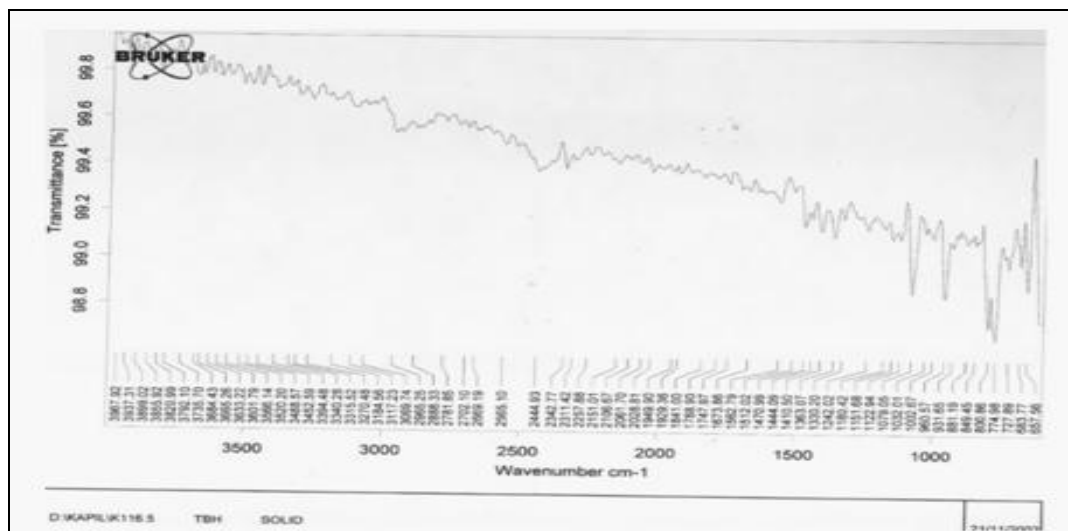


FIG. 2: IR SPECTRUM OF TBH

TABLE 1: IR SPECTRA HAVING WAVE NUMBER RANGE WHICH SHOWS SIGNAL ASSIGNMENT OF DRUGS

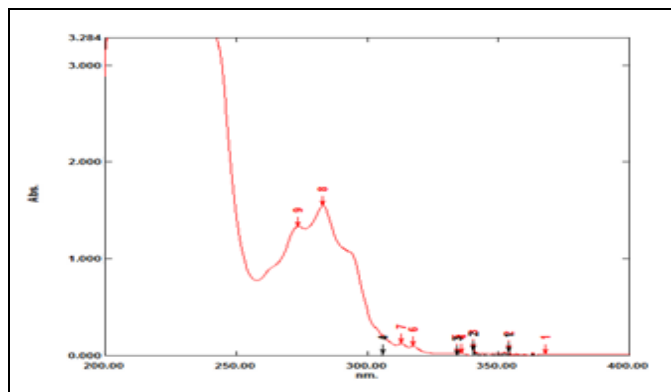
S. no.	Functional Group	Wave Number (cm ⁻¹)	Observation (cm ⁻¹)
1	OH stretching	3200 - 2800	3069.74
2	SH stretching	2800 - 2400	2444.93
3	CN stretching	2400 - 2000	2342.77
4	C=O stretching	1800 - 1600	1633.76
5	CH bending	1600 - 1400	1470.99
6	COOH stretching	1400 - 1200	1363.07
7	S=O stretching	1200 - 1000	1079.05
8	CH bending	1000 - 800	800.86
9	C-Cl stretching	800 - 600	774.98

Solubility Characteristics: Qualitative solubility of the drug was checked in various solvents and found that the drug was freely soluble in methanol and insoluble in chloroform, sparingly soluble in 0.1 N HCl, slightly soluble in water. The result demonstrated in **Table 2** was found that the drug Terbinafine HCl is lipophilic in nature because it was soluble in an organic solvent.

TABLE 2: SOLUBILITY STUDY OF TERBINAFINE HYDROCHLORIDE IN DIFFERENT SOLVENTS

S. no.	Solvents	Inform	Observed Solubility
1	Methanol	++++	Freely soluble
2	Ethanol	+++	Soluble
3	Water	+	Sparingly soluble
4	0.1 HCl	+	Sparingly soluble
5	Chloroform	---	Insoluble

U.V. Spectrum: Spectrum of TBH for 3 µg/ml in 50% aqueous methanol was recorded between 200 - 400 nm. Spectrum for above concentration was obtained with n = 3 and was recorded at 283 nm, which is shown in **Fig. 3**.

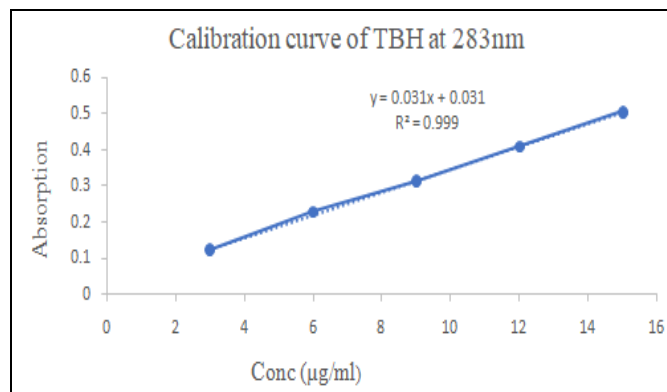
**FIG. 3: SPECTRUM OF TERBINAFINE HYDROCHLORIDE IN 50% AQUEOUS METHANOL**

Calibration Curve: Appropriate volume of aliquots from standard Terbinafine Hydrochloride stock solutions were transferred to different volumetric flasks of 10 ml capacity. The volume was adjusted to the mark with the methanol to

obtain a concentration of 3, 6, 9, 12, and 15 µg/ml. Absorbance at 283 nm was measured, and the plot of absorbance vs. concentration was plotted. The straight-line equation was determined as: $y = 0.0316x + 0.0319$ which is & illustrated in **Table 3** & shown in **Fig. 3a**.

TABLE 3: CALIBRATION READINGS AT 283 nm FOR TERBINAFINE HYDROCHLORIDE IN 50% AQ. METHANOL

Conc. (µg/ml)	Absorbance			
	n=1	n=2	n=3	Avg. n=3abs
3	0.118	0.128	0.125	0.123
6	0.199	0.250	0.240	0.229
9	0.320	0.312	0.310	0.314
12	0.419	0.399	0.412	0.410
15	0.516	0.495	0.510	0.507

**FIG. 3A: CALIBRATION CURVE FOR TERBINAFINE HYDROCHLORIDE (3 – 15 µg/ml) AT 283 nm**

Images of Prepared Scaffolds:

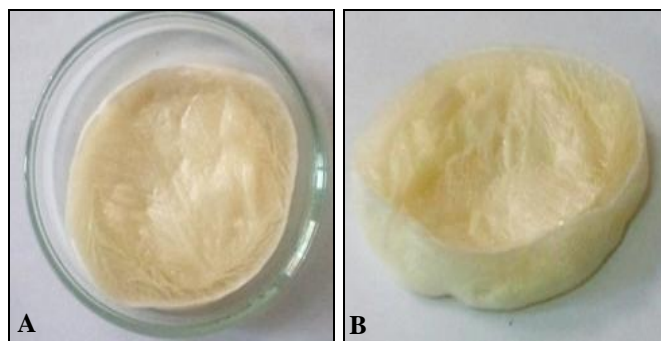
**FIG. 4A, B: 3D POROUS CHITOSAN SCAFFOLD**



FIG. 4C: CHITOSAN COMPOSITE TBH SCAFFOLD

Measurement of pH of CH/TBH Composite Slurry: The apparent pH of the slurry was determined using pH meter (pH Tutor Bench Meter, EUTECH Instruments, Singapore) in triplicate at 25 °C, pH of the CS/TBH composite gelled was found to be 6.59 ± 0.06 . The pH of the CS mixed TBH gel was within the acceptable range for topical scaffold preparations and compatible with the pH of the skin.

Rheological behavior of CS/TBH Composite Solution: The flow behavior of a polymer composite solution CS/TBH has been reported. Viscosity was analyzed for the CS/TBH slurry under varied shear stress shown in Fig. 5. The solution has shown Non-Newtonian behavior with shear-thinning ability of composite solution (TBH 1% wt. /wt.). CS/TBH solution has shown viscosity 1.20Pa at a shear rate of 100 cm^{-3} illustrated in Table 4. Altered in viscosity has an impact on the pore size of the developed scaffold, as reported earlier? Depending on where and how the preparation procedure is done, the molecular weight may change from 300 to over 1000 kD, viscosity and molecular weight are inversely proportional to the degree of acetylation. Therefore, the greater the molecular weight is, the chitosan membranes tend to be more viscous, thus allowing for controlling fluidity in them, an important

feature in tissue interaction. Due to its high molecular weight and its lineal nonbranched structure, chitosan is a strong viscosity-building agent in acid mediums and behaves as a pseudoplastic material, where viscosity depends on agitation.

TABLE 4: APPARENT VISCOSITY AT DIFFERENT SHEAR RATE

S. no.	Shear rate (cm^{-1})	Apparent viscosity (Pa)
1	40	3.8
2	50	3.4
3	60	2.7
4	70	2.4
5	80	2.1
6	90	1.6
7	100	1.2

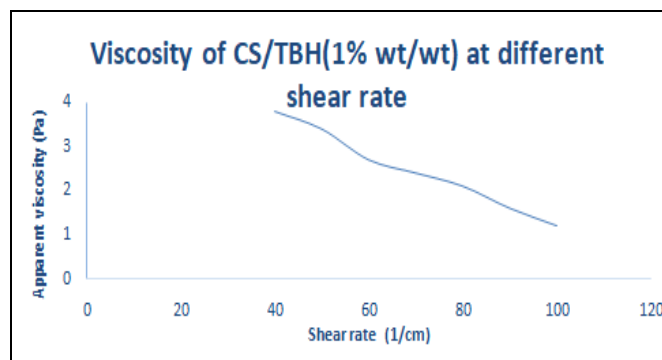


FIG. 5: RHEOLOGICAL BEHAVIOUR OF CS/TBH SOLUTION. SOLUTION SHOWS NON-NEWTONIAN BEHAVIOUR WITH SHEAR THINNING PROPERTY

Thermal Characterization (DSC): Chitosan and Terbinafine HCL showed an endothermic peak at 210 °C and 103 °C shown in Fig. 6a and Fig. 6b respectively. The combination of Chitosan and Terbinafine HCl showed a peak at 196 and 101, as shown in Fig. 6c. From the DSC study, it has been cleared that there are no significant changes in polymer and drug melting peak. From the DSC results, it has been concluded that the drugs and polymer are compatible with each other and selected for further formulations studies.

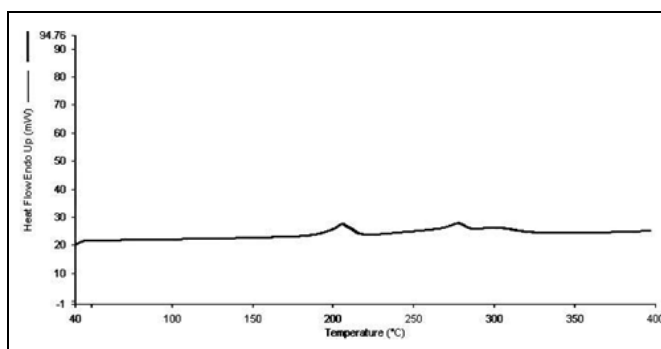


FIG. 6A: DIFFERENTIAL SCANNING CALORIMETRY OF CHITOSAN

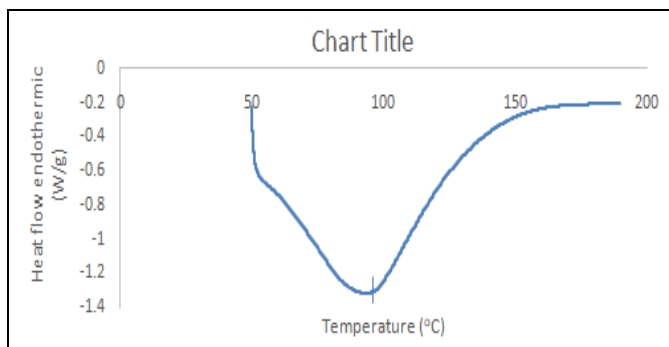


FIG. 6B: DSC SPECTRA OF TERBINAFINE HCl

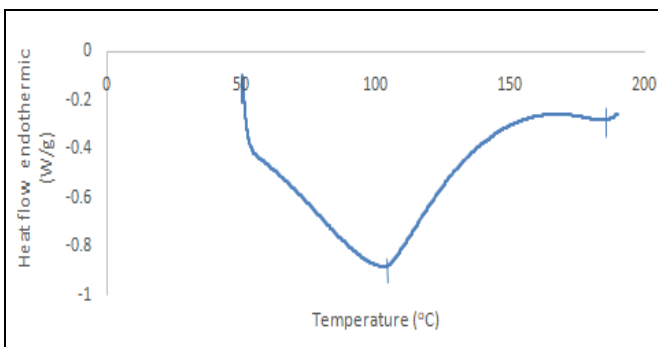


FIG. 6C: DSC SPECTRA OF TBH AND CHITOSAN MIXTURE

TABLE 5: THICKNESS AND DIAMETER OF PREPARED SCAFFOLDS

Num.of scaffold	Parameters (mm)	
	Thickness	Diameter
1	4.54 ± 0.2	24.2 ± 0.5
2	4.57 ± 0.6	25.9 ± 0.3
3	4.57 ± 0.4	25.4 ± 0.1
Average	4.52 ± 0.4	25.16 ± 0.3

Thickness and Diameter of CS/TBH Composite Scaffolds: Thickness and diameter of the scaffold were measured by Digital Vernier Caliper (150 mm), which are illustrated in Table 5. Three parallel sets were analyzed for each character, and the mean value of the thickness and diameter of different scaffolds were noted as 4.52 ± 0.4 mm and 25.16 ± 0.3 mm, respectively.

Morphology and Pore Size: Adequate pore size and interconnectivity of pores in scaffolds are vital factors for the diffusion of oxygen and drugs to the cells and foster transfer of metabolic wastes.

SEM images are shown in Fig. 7a & 7b were taken to visualize these features. SEM analysis showed for both pure CS and CS/TBH composite scaffolds did have uniform porosity with pore size ranging from 50 μm to 200μm, respectively. This pore size range is very beneficial for cell growth. These interconnected pores are required for the cells to communicate freely while scaffolds are being used for tissue engineering.

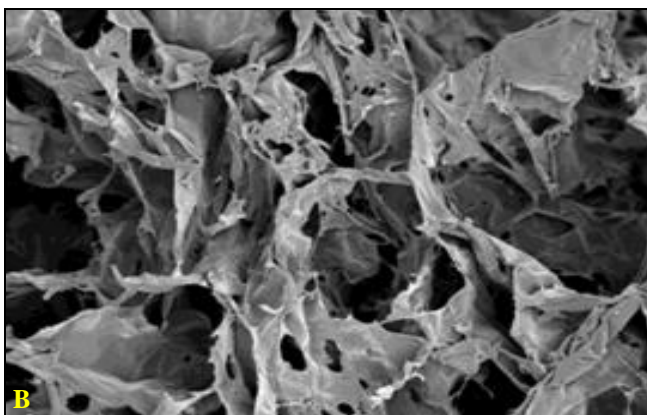
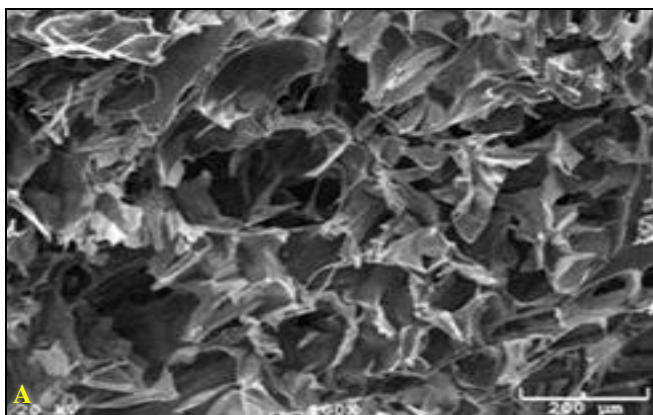


FIG. 7A & B: SEM IMAGES OF CS/TBH COMPOSITE SCAFFOLD. THE SCALE BAR REPRESENTS 200 μm: IMAGE TAKEN AT 100X MAGNIFICATION

Porosity: The porosity of the scaffold is an important factor that decides not only the transport of nutrients required for cell growth but also drug infiltration and migration. The total porosity of the pure CS scaffold and CS/TBH composite scaffold were estimated using the liquid displacement method. The porosity of the chitosan scaffold was found 83.3%, whereas, by the addition of TBH (1%) in the polymeric matrix, it was found 80.2%, which are shown in Table 6.

TABLE 6: % POROSITY OF PURE CHITOSAN AND CS/TBH SCAFFOLD

No. of sample (n)	% Porosity	
	Pure Chitosan scaffold	CS/TBH scaffold
1	82.3	79.3
2	83.2	80.1
3	84.4	81.2
Average value n=3	83.3	80.2

The addition of TBH had no major change in porosity. However, the small reduction in porosity

indicates improved apparent density. High density could contribute to high mechanical strength, and optimal porosity is a measure of permeability. Hence, TBH has an accepted role in attaining a balance between porosity and density of the scaffold.

Apparent Density: Average apparent density of CS/TBH was found to be 0.156 g/cm³, which was within the optimal range as shown in **Table 7**: Average density of pure CS scaffold was found to be 0.11 g/cm³. Higher density contributes to higher mechanical strength. Hence, this suggests that CS/TBH scaffold has an acceptable density.

TABLE 7: AVERAGE APPARENT DENSITY OF SCAFFOLDS

Average weight (g) n=3		Average apparent density (g/cm ³) n=3	
CS scaffold	CS/TBH scaffold	CS scaffold	CS/TBH scaffold
0.262	0.362	0.112	0.156

Swelling Ability: The degree of swelling of scaffolds in PBS was analyzed in triplicate form for 28 days. The swelling pattern for the CS/TBH composite scaffold on the different time periods is shown in **Fig. 8a** and found 11.34 as illustrated in **Table 8**, which were same at different time periods.

There were no significant changes in swelling ratio from its 1st day to 28th day, which shows favorable three-dimensional environments for the constant drug diffusion and provides acceptable structural integrity.

TABLE 8: AVERAGE DRY WEIGHT AND WET WEIGHT

Average DRY wt. scaffold (g)	Average WET wt. scaffold (g)
0.362	4.47
Swelling ratio [(WET wt. - DRY wt.) / DRY wt.] = 11.34	

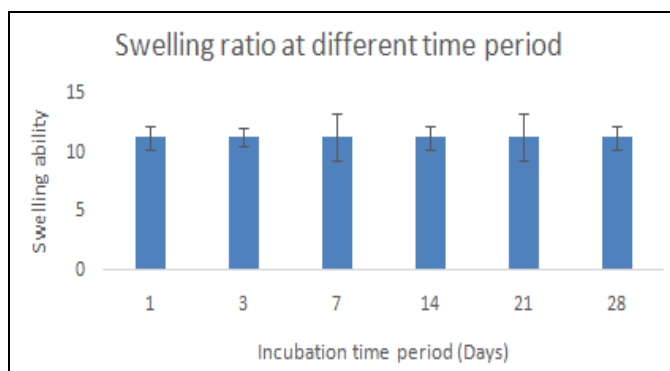


FIG. 8A: SWELLING RATIO OF CS/TBH SCAFFOLDS IN PBS

Swelling behavior of the scaffold during 24 h of time had also been studied and observed that during an initial period (5-6 h) of the experiment, a rapid increase in swelling is prominent beyond which the scaffolds show a saturated swelling without any further change in % swelling. The swelling pattern for the first 24 h has shown in **Fig. 8b**.

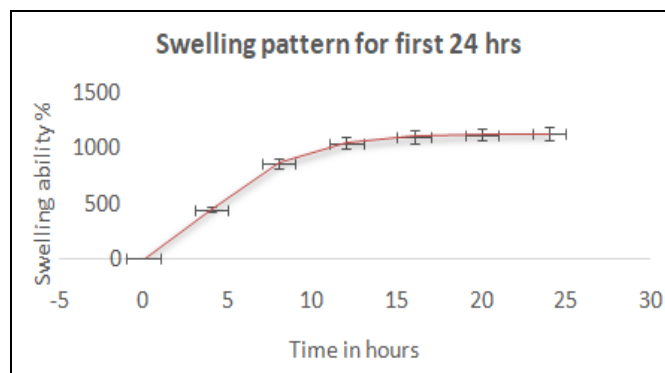


FIG. 8B: SWELLING BEHAVIOUR OF SCAFFOLD FOR INITIAL 24 h

Water Retention Ability: The retention ability of chitosan/TBH composite scaffold after 24 h with the value mean ±SD (n=3) was found 521.54%, as illustrated in **Table 9**.

TABLE 9: AVERAGE DRY WEIGHT AND AVERAGE WET WEIGHT SCAFFOLD

Average W _{dry} scaffold (g)	Average W _{wet} scaffold (g)
0.362	2.250
Retention ability(E _R) = [(W _{wet} - W _{dry}) / W _{dry}]/100 = 521.54%	

FTIR Analysis: An infrared spectrum represents the characteristics of a material with absorption bands. Thus infrared spectroscopy can provide positive identification of every different constituent present in the composite matrices.

FT-IR analysis of CS and CS/TBH composite scaffolds was, therefore, done to evaluate the interaction between the individual components present in the scaffolds. The characteristics peak of TBH and chitosan liquid mixture are shown in **Fig 9b**.

Comparing the spectra of an aqueous mixture of chitosan/TBH and pure chitosan spectra are shown in **Fig. 9a** revealed that there were no significant changes in the IR spectral pattern of drug-polymer mixture, which indicated the absence of interaction between drug and polymer. **Table 10** reports the graph on the basis of individual functional group.

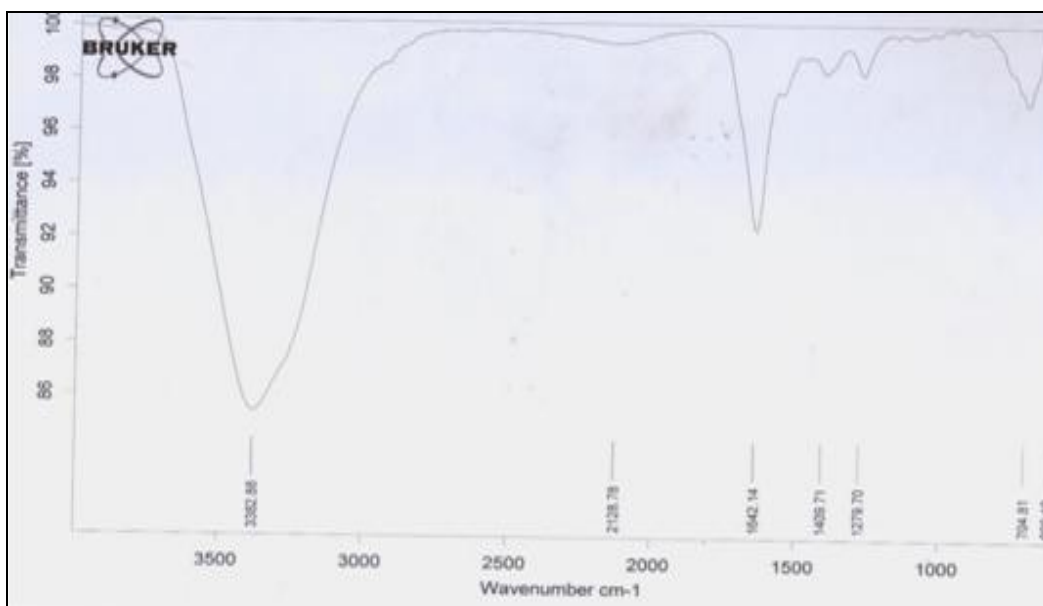


FIG. 9A: IR SPECTRUM OF PURE CHITOSAN AQUEOUS SOLUTION

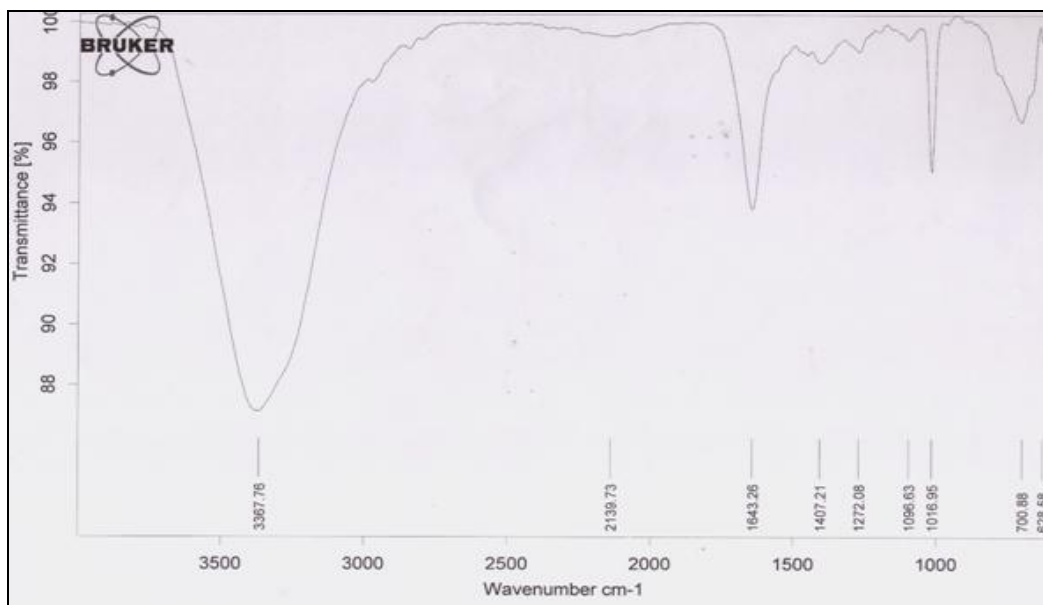


FIG. 9B: IR SPECTRUM OF CHITOSAN/TBH AQUEOUS MIXTURE

TABLE 10: FTIR PEAKS OF PURE CHITOSAN AND CHITOSAN/TBH

Description	Functional groups	Characteristics of peak cm ⁻¹
Chitosan pure	OH-	3382.88
	C=O	1642.14
	NH	1409.71
	C-C	1279.70
	C-O	704.81
Chitosan and TBH composite		3367.78, 1643.26, 1407.21, 1272.08, 700.88 and 1016.95
Report: - No any significant differences in the position of absorption bands were seen; minor deviation in band were observed which might be expected as an instrumental error. Moreover, the characteristics of absorption bands at 1016.95 corresponded to TBH.		

Optical Microscopy: The optical microscopic image of CS/TBH composite scaffold clearly indicated that the scaffold has a pore structure. The 2D calibration of scaffold showed pore diameter ranging from 150 to 200 μm, as shown in **Fig. 10b & c**. The optical microscopic image of CS/TBH

shows the dispersed status of drug TBH in the matrix with the slight aggregation of TBH, as shown in **Fig. 10a**. This indicated that the TBH drugs are distributed within the chitosan matrix; these results were consistent with the SEM observations.

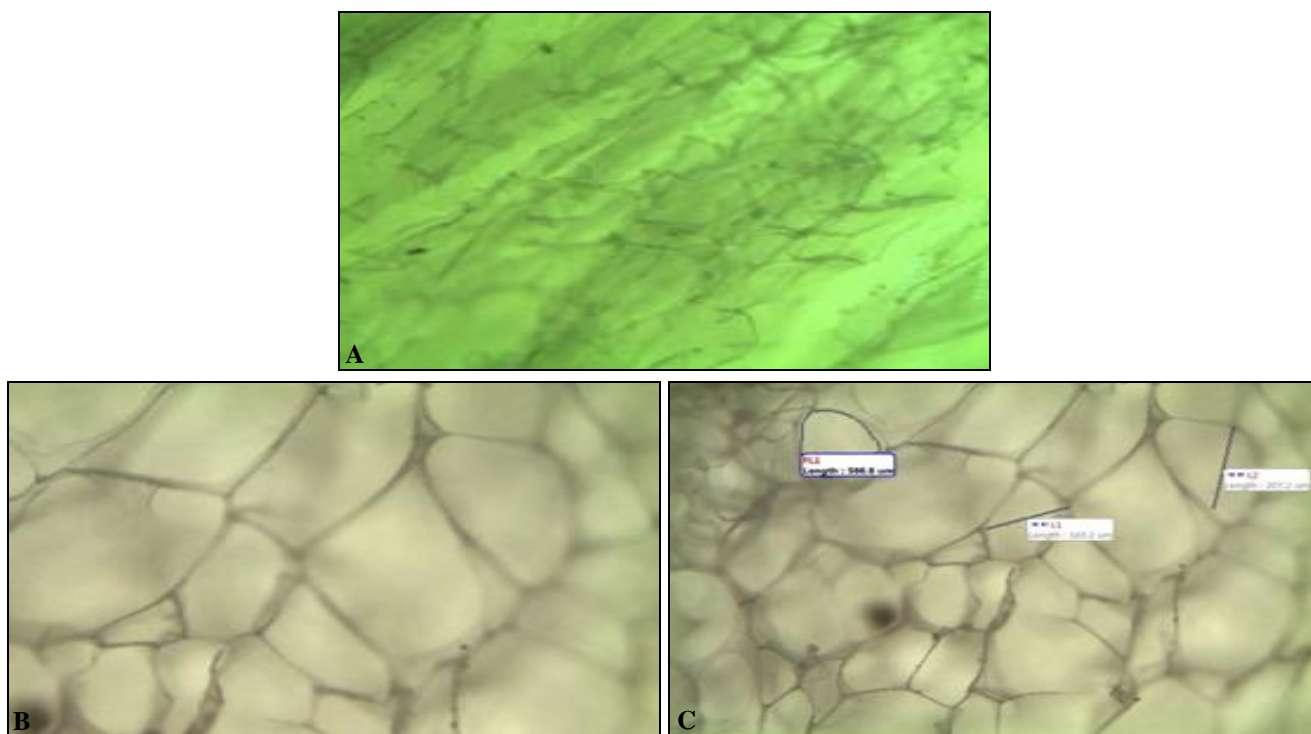


FIG. 10A, B, C: OPTICAL MICROSCOPIC IMAGES OF SCAFFOLDS ON DIFFERENT MAGNIFICATION POWER

In-vitro Biodegradation Study: The degradation of scaffolds is one of the major goals of tissue engineering research because of the self-repairing ability of various tissues are different implying that scaffold should have corresponding degradation rates to facilitate new tissue synthesis. So, adequate control over the rate of degradation plays a major role to be on part with the growth rate of new tissue formed. Therefore, biodegradation of the prepared CS/TBH composite scaffolds was studied in phosphate buffer saline containing Lysozyme for five weeks and found around 45% weight loss after 35 days, which is shown in Fig. 11 and reading tabulated in Table 11.

TABLE 11: SHOWS % WEIGHT REMAINING AFTER DIFFERENT DAY'S INTERVAL

Days	Weight after Incubation (W _F) (g)	% Weight loss	% Weight remaining (100- % weight loss)
2 nd	0.347	4	96
7 th	0.320	10	90
14 th	0.271	25	75
21 st	0.235	35	65
28 th	0.217	40	60
35 th	0.199	45	55

A scaffold's ability to degrade in concert with new tissue formation is a major parameter in scaffold design for tissue regeneration, which could be attributed to an increase in hydrophilicity of the composite by any means.

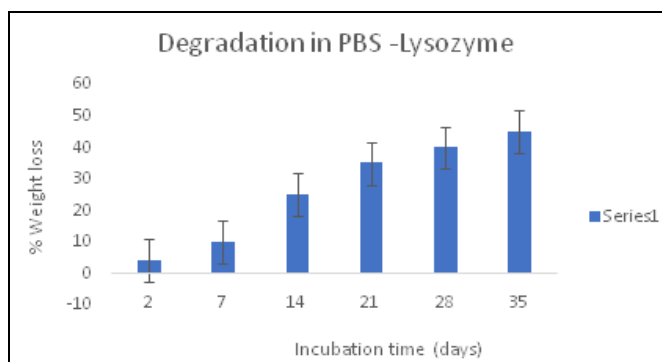


FIG. 11: DEGRADATION PATTERN OF CS/TBH SCAFFOLD IN DIFFERENT DAY'S INTERVAL

In-vitro Drug Release: The *in-vitro* release profile curves obtained by the dialysis method from TBH loaded Chitosan scaffold were investigated in PBS, pH 7.4 at 37 °C over 18 h. It was found that in the initial 2 h, 4.38 ± 2.9% of drug became available. However, after 4 h, the drug release from scaffold was 9 ± 3.9%, which began to improve gradually.

The drug release from the CS composite scaffold demonstrated monophasic trend characterized by slow release of a drug that can be as outcomes of the time taken for wetting the scaffold under initial condition. After 16 h of evaluation 92.15 ± 7.4% of the drug was available from Chitosan/TBH scaffold, which is shown in Fig. 12 and reading tabulated in Table 12.

Hence, our investigation ensured that the drug release from the scaffold was prolonged and effective in comparison to marketed cream which has 94.7% after 8 h as per the investigation reported by Kaushal R. Sabu *et al.*²¹

Prolonged drug delivery mediated by the chitosan scaffold can be beneficial in limiting the fungal induced wound for an extended time and also minimize the rate of reapplication that contributes to effective wound healing and treatment.

TABLE 12: % CUMULATIVE DRUG RELEASE AT DIFFERENT TIME INTERVALS

S. no.	hrs	abs	corr abs	conc ug/ml	*4	*30	cumm	mg	% cdr
1	1	0.1	0.1	2.15506	8.62025	258.608	258.608	0.25861	2.58608
2	2	0.12	0.145	3.57911	14.3165	429.494	438.114	0.43811	4.38114
3	4	0.15	0.28	7.85127	31.4051	942.152	965.089	0.96509	9.65089
4	6	0.22	0.4775	14.1013	56.4051	1692.15	1746.49	1.74649	17.4649
5	8	0.27	0.695	20.9842	83.9367	2518.1	2628.85	2.62885	26.2885
6	10	0.34	0.9975	30.557	122.228	3666.84	3861.52	3.86152	38.6152
7	12	0.41	1.355	41.8703	167.481	5024.43	5341.34	5.34134	53.4134
8	14	0.49	1.7925	55.7152	222.861	6685.82	7170.215	7.17022	71.7022
9	16	0.54	2.2725	70.9051	283.62	8508.61	9215.861	9.21586	92.1586

TBH release from chitosan polymeric matrix via dialysis bag membrane. 100 mg drug was loaded in the chitosan scaffold.
Reservoir: 30 ml PBS

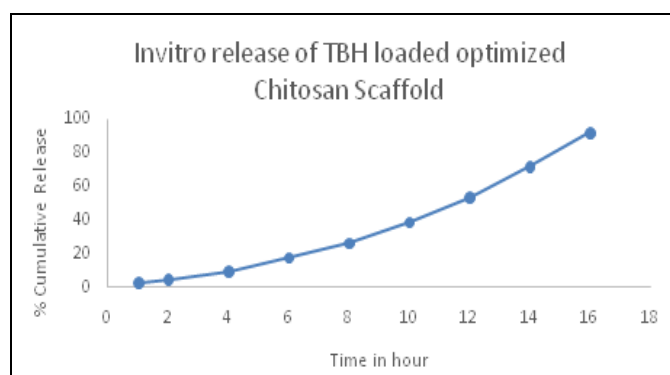


FIG. 12: IN-VITRO DRUG PROFILE OF TBH FROM CHITOSAN POLYMERIC SCAFFOLD IN SIMULATED WOUND FLUID (SWF), pH 7.4, MAINTAINED AT 37 °C

CONCLUSION: TBH loaded CS scaffold was prepared and optimized to make it compatible with the tissue for the composite actions against the fungal impaired wound. The optimized scaffolds formulation exhibited porous morphology with optimum pore size, prolonged and effective drug release without any drug-polymer interaction & had good biodegradability, biocompatibility, optimum swelling ability, and porosity.

Optimum porosity indicates better permeability. Overall, data suggest alternative and potential promising therapeutic options for the management of fungal induced wounds. Future studies on an animal will reveal the potential properties in aspect with accelerative fungal wound healing.

Suggested Future Work: The following research works are suggested for future study with the developed composite scaffolds.

- Three-dimensional scaffolds with appropriate design may be fabricated by adopting advanced scaffold fabrication technique like electrospinning, rapid prototyping methods.
- Angiogenesis study can be performed to confirm the vascularization aspect of the developed scaffold.
- In-vivo* animal study can be undertaken for assessing its therapeutic efficacy for recommended fungal wound healing and its future alternative clinical application.

ACKNOWLEDGEMENT: Mr. Roshan P. Yadav conceptualized and gathered the data with regard to this work. Dr. Meenakshi K. Chauhan analyzed these data, and necessary inputs were given towards the designing of the manuscript. Both authors discussed the methodology and results and contributed to the final manuscript.

CONFLICTS OF INTEREST: The authors confirm that this research article content has no conflict of interest.

REFERENCES:

- Mow VC and Huiskers R: Basic orthopedic biomechanics and mechano-biology, Lippincott Williams & Wilkins, 2005.
- Martins M: Responsive and in situ-forming chitosan scaffolds for bone Tissue engineering applications: an overview of the last decade. Journal of Materials Chemistry 2010; 20: 1638-45.

3. Mohammadi Y: Osteogenic differentiation of mesenchymal stem cellson novel three-dimensional poly (l-lacticacid)/chitosan/gelatin/beta-tricalcium phosphate hybrid scaffolds. Iranian Polymer Journal 2007; 16: 57.
4. Sabir MI: A review o biodegradable polymeric materials for bone tissue engineering applications. Journal of Materials Science 2009; 44: 5713-24.
5. Yunfeng L: Review on techniques of design and manufacturing for bone tissue engineering scaffold. On Biomedical Engineering and Informatics, 2009. BMEI'09.2nd International Conference on 2009; 1-4.
6. Stroncek JD and Reichert WM: Overview of wound healing in different tissue types. In dwelling Neural Implants: Strategies for contending with the in vivo environment, 2008.
7. Venkatesan J and Kim SK: Chitosan composites for bone tissue engineering-An overview. Marine drugs 2010; 8: 2252-66.
8. Ruiran H: Preparation of β -calcium phosphate/chitosan composite scaffolds and its effect on osteoblasts behavior. Journal of Functional Materials 2010; 41: 148-51.
9. Dutta PK: Chitin and chitosan: Chemistry, properties and applications. Journal of scientific and Industrial Research 2004; 63: 20-31.
10. Li Z: Chitosan–alginate hybrid scaffolds for bone tissue engineering. Biomaterials 2005; 26: 3919-28.
11. De Groot J: Use of porous polyurethanes formeniscal reconstruction and meniscal prostheses. Biomaterials 1996; 17: 163-73.
12. Salgado AJ: Bone tissue engineering: state of the art and future trends. Macromolecular Bioscience 2004; 4: 743-65.
13. Barbosa M: Polysaccharides as scaffolds for bone regeneration. Itbm-Rbm 2005; 26: 212-17.
14. Sultana N and Kadir MRA: Study of *in-vitro* degradation of biodegradable polymer based thin films and tissue engineering scaffolds. African Journal of Biotechnology 2013; 10: 18709-715.
15. Dorati R: Effect of porogen on the physicochemical properties and degradation performance of PLGA scaffolds. Polymer Degradation and Stability 2010; 95: 694-01.
16. Kumari B and Kesavan K: “ffect of chitosan coating on micro emulsion for effective dermal clotrimazole delivery. Pharmaceutical Development and Technology, 30 Aug 2016
17. Marino G: β -Tri calcium phosphate 3D scaffold promote alone osteogenic differentiation of human adipose stem cells: *in-vitro* study. Journal of Materials Science: Materials in Medicine 2010; 21: 353-63.
18. Li C: Bone morphogenetic protein-9 induces osteogenic differentiation of rat dental follicle stem cells in P38 and ERK1/2 MAPK dependent manner. International Journal of Medical Sciences 2011; 9: 862-71.
19. Dewangan A and Tomar B: International Journal of Pharmaceutical and Biological Sciences Archive 2013; 1(2): 36-52.
20. Baldino L and Cardea S: Chitosan scaffolds formation by a supercritical freeze extraction Process. The Journal of Supercritical Fluids 2014; 90: 27-34.
21. Sabu KR and Basarkar GD: Formulation Development and In-vitro Evaluation of Terbinafine HCL Emulgel for Topical Fungal Infection. Int J Pharm Sci Rev Res 2013; 21(2): 168-73.
22. Zhao L: Preparation and HL-7702 cell functionality of titanium/chitosan composite scaffolds. Journal of Materials Science: Materials in Medicine 2009; 20: 949-57.
23. Gaba B and Fazil M: Nanostructured lipid carrier system for topical delivery of Terbinafine Hydrochloride.” Bulletin of Faculty of Pharmacy, Cairo University 2015; 53(2): 147-59.
24. ozcan I, Abact O and Uztan AH: Enhanced topical delivery of terbinafine hydrochloride with chitosan hydrogel’s. AAPS Pharm SciTech, Vol. 10, 2009.
25. Mohiti-Asli M and Pourdeyhimi B: Novel, silver-ion-releasing nano fibrous scaffolds exhibit excellent antibacterial efficacy without the use of silver nanoparticles. Acta Biomaterialia 2014; 10(5): 2096-04.
26. Karri VVSR and Kuppusamy G: Curcumin loaded chitosan nanoparticles impregnated into collagen –alginate scaffolds for diabetic wound healing. International Journal of Biological Macromolecules 2016; Part B: 1519-29.
27. New N and Furuike T: The mechanical and biological properties of chitosan scaffolds for tissue regeneration templates are significantly enhanced by chitosan from *Gongronella butleri*. Materials 2009; 2: 374-98.
28. Kavya KC, Jayakumar R and Nair S: Fabrication and Characterization of chitosan/gelatin/nSiO₂ composite scaffold for bone tissue engineering. International Journal of Biological Macromolecules 2013; 59: 255-63.
29. Patil F: Osteoblastic cellular responses on ionically cross linked chitosan-tripolyphosphate fibrous 3-D mesh scaffolds. Journal of Biomedical Materialia Research 2013; 101.
30. Adhikari U, Rijal NP and Khanal S: “Magnesium incorporated chitosan based scaffold for tissue engineering applications. Bioactive Materials 2016; 132-39.
31. Venkatesan J and Ryu B: Preparation and Characterization of chitosan- carbon nanotube scaffolds for bone tissue engineering. International Journal of Biological Macromolecules 2012; 50: 393-02.

How to cite this article:

Yadav RP and Chauhan MK: Terbinafine loaded chitosan scaffold for fungal wound treatment. Int J Pharm Sci & Res 2020; 11(8): 3806-18. doi: 10.13040/IJPSR.0975-8232.11(8).3806-18.

All © 2013 are reserved by the International Journal of Pharmaceutical Sciences and Research. This Journal licensed under a Creative Commons Attribution-NonCommercial-ShareAlike 3.0 Unported License.

This article can be downloaded to **Android OS** based mobile. Scan QR Code using Code/Bar Scanner from your mobile. (Scanners are available on Google Playstore)